

# Variable projection without smoothness

A.Y. Aravkin, D. Drusvyatskiy, and T. van Leeuwen

**Abstract**—The variable projection technique solves structured optimization problems by completely minimizing over a subset of the variables while iterating over the remaining variables. Over the last 30 years, the technique has been widely used, with empirical and theoretical results demonstrating both greater efficacy and greater stability compared to competing approaches. Classic examples have exploited closed form projections and smoothness of the objective function. We apply the idea in broader settings, where the projection subproblems can be nonsmooth, and can only be solved inexactly by iterative methods. We illustrate the technique on sparse deconvolution and robust machine learning applications. Open source code for nonsmooth variable projection is available through github<sup>1</sup>.

**Index Terms**—Variable projection, nonsmooth optimization.

## I. INTRODUCTION

In this paper, we consider optimization problems of the form

$$\min_{x, \theta} g(x, \theta) + h(\theta) + r(x), \quad (1)$$

where  $g : \mathbb{R}^k \times \mathbb{R}^n \rightarrow \mathbb{R}$  is smooth, and  $h$  and  $r$  are convex (but possibly non-smooth). In particular, we target applications in signal-processing, high-dimensional statistics and machine learning. Here,  $x$  is viewed as a variable of primary interest, while  $\theta$  represents a set of auxiliary (nuisance) parameters. In many applications, efficient algorithms have been developed to globally minimize the objective function in  $x$  for fixed  $\theta$ . We provide a provably convergent algorithmic recipe to extend these algorithms to (1).

We begin by reviewing the classic *Variable Projection* (VP) technique for nonlinear least squares problems. Early work on the topic [10] has found numerous applications in chemistry, mechanical systems, neural networks, and telecommunications (see the surveys of [11] and [15], and references therein.) Consider the *separable nonlinear least-squares problem* [11], [15],

$$\min_{x, \theta} f(x, \theta) := \|\Phi(x)\theta - y\|_2^2, \quad (2)$$

where the matrix-valued map  $\Phi(x) \in \mathbb{C}^{m \times n}$  is smooth and has full rank for each  $x$ . Let us formally eliminate the variable  $\theta$  by introducing

$$\tilde{f}(x) = \min_{\theta} \|\Phi(x)\theta - y\|_2^2. \quad (3)$$

The function  $\tilde{f}(x)$  can be explicitly evaluated, since  $f(x, \cdot)$  is a convex quadratic in  $\theta$ . More precisely, we have  $\tilde{f}(x) = f(x, \theta(x))$  with

$$\theta(x) = \Phi(x)^\dagger y,$$

where  $\Phi(x)^\dagger$  denotes the Moore-Penrose pseudoinverse of  $\Phi(x)$ . The VP technique solves (2) by running an iterative solver on  $\min_x \tilde{f}(x)$  [10], with  $\nabla \tilde{f}(x)$  computed using the formula

$$\nabla \tilde{f}(x) = \nabla_x f(x, \theta)|_{x, \theta(x)}.$$

Second-order information of  $\tilde{f}(x)$  can also be obtained through the Schur complement of the Hessian  $\nabla^2 f(x, \theta)$  [6]. For example, [23] showed that when the Gauss-Newton method for (2) converges superlinearly, so do Gauss-Newton variants for (3).

The underlying principle applies more broadly. For example, the authors of [4], [6] apply the VP technique to (1) when  $g$  is a  $C^2$ -smooth function and  $r = 0$ ,  $h = 0$ . Variable projection in the general context of (1) refers to partial minimization in  $\theta$ . This operation is sometimes also called *epigraphical projection* [20, Proposition 1.18].

**Contribution.** We show how to apply the variable projection technique to *nonsmooth* problems of the form (1). To this end, define the reduced function

$$\tilde{f}(x) := \min_{\theta} g(\theta, x) + h(\theta), \quad (4)$$

and its slightly regularized variant

$$\tilde{f}_\beta(x) := \min_{\theta} g(\theta, x) + h(\theta) + \frac{\beta}{2} \|\beta\|_2^2.$$

We present conditions that ensure  $\tilde{f}$  and/or  $\tilde{f}_\beta$  are differentiable. We then develop a provably convergent algorithm for (1) that evaluates  $\tilde{f}$  and  $\nabla \tilde{f}$  in (4) approximately by solving the associated problems (4) inexactly.

The outline of the paper is as follows. In Section II, we present a survey of nonsmooth applications: exponential fitting, sparse deconvolution, and robust learning formulations. In Section III, we develop derivative formulas for the nonsmooth case (4), and outline an algorithmic framework for solving the problem (1) using inexact solves of the inner problem in  $\theta$ . In section IV, we return to the problems outlined in section II and present numerical results. Conclusions complete the paper.

<sup>1</sup><https://github.com/UW-AMO/VarProNonSmooth>

## II. NONSMOOTH VARIABLE PROJECTION IN APPLICATIONS

In this section, we describe three classes of applications where nonsmooth VP plays a central role: exponential data fitting, robust inference, and multiple kernel learning.

### A. Robust and sparse exponential data-fitting

Exponential data-fitting is one of the most common applications of the variable projection technique [18]. The data generating mechanism is given by

$$y_i = \sum_{j=1}^n \theta_j \exp(-\varphi_{ij}(x)),$$

where  $\theta \in \mathbb{R}^n$  are unknown weights,  $y \in \mathbb{R}^m$  are the observed measurements, and  $\varphi_{ij}$  are known functions that depend on an unknown parameter  $x \in \mathbb{R}^k$ . Some examples of this class are given in table I.

Introducing the matrix  $\Phi(x)$  with entries  $\Phi(x)_{ij} := \exp(-\varphi_{ij}(x))$ , we express the noisy measurements as

$$y = \Phi(x)\theta + \epsilon.$$

A natural approach is then to formulate a nonlinear least squares problem,

$$\min_{\theta, x} \|\Phi(x)\theta - y\|_2^2,$$

which is readily solved using the classic VP algorithm. In practice, we may not know the correct number of terms  $n$  to include in the sum. Choosing a large value for  $n$  may lead to unreliable estimates and poor generalizability. To obtain a more parsimonious solution, we can include a sparsity-inducing prior on  $\theta$ :

$$\min_{\theta, x} \rho(\Phi(x)\theta - y) + \lambda \|\theta\|_1,$$

where  $\lambda > 0$  is a penalty parameter. Additional constraints on  $\theta$  may be added [16], [29]. When measurements are contaminated by outliers, we may also want to use a robust penalty  $\rho$  on the residual, rather than the sum of squares.

### B. Multiple Kernel Learning

Kernel methods are a powerful technique in classification and prediction [28], [30]. Given a set of  $k$  samples  $a_i \in \mathbb{R}^N$  and corresponding labels  $y_i \in \mathbb{R}$ , the goal is to classify new samples. Let  $\Phi(\cdot) : \mathbb{R}^N \rightarrow \mathcal{H}$  be a pre-defined transformation that sends  $a_i$  into a Reproducing Kernel Hilbert Space (RKHS) [24], [27]. We then look for a hyperplane  $(z, \alpha)$  such that  $\text{sign}(\langle z, \Phi(a_i) \rangle + \alpha) \approx y_i$ , and use  $(z, \alpha)$  to classify new samples. This problem can be formalized as follows

$$\min_{z \in \mathcal{H}, \alpha \in \mathbb{R}} \frac{1}{2} \|z\|_{\mathcal{H}}^2 + C \sum_{i=1}^k (1 - y_i (\langle z, \Phi(a_i) \rangle + \alpha))_+,$$

with  $r_+ = \max(r, 0)$ . The dual to this problem is a finite dimensional quadratic program (QP):

$$\min_{x \in [0, C]^k} \frac{1}{2} \|x\|_K^2 - 1^T x \quad \text{s.t.} \quad x^T y = 0, \quad (5)$$

where  $K$  is the *Kernel matrix* given by  $K_{ij} := y_i y_j \langle \Phi(a_i), \Phi(a_j) \rangle$ . Once the dual is solved,  $z$  is recovered via

$$z = \sum_{i=1}^k x_i y_i \Phi(a_i),$$

with several strategies available to recover  $\alpha$ , see e.g. [30]. Since  $\mathcal{H}$  may be infinite-dimensional, its convenient that the prediction function takes the form

$$\begin{aligned} \hat{y} &= \text{sign}(\langle z, \Phi(a) \rangle + \alpha) \\ &= \text{sign} \left( \sum_{i=1}^k x_i y_i \langle \Phi(a_i), \Phi(a) \rangle + \alpha \right). \end{aligned}$$

The choice of kernel is an art-form; there are many options available, and different kernels perform better on different problems. To develop a disciplined approach in this setting, *multiple kernel learning* (MKL) has been proposed. Given  $n$  kernels functions  $\Phi_i$  with corresponding kernels  $K_i$ , consider the weighted linear combination

$$K(\theta) = \sum_{i=1}^n \theta_i K_i.$$

A natural question is to find the best weights  $\theta$  [19]. Requiring  $\theta$  to be in the unit simplex yields the problem

$$\min_{\theta \in \Delta_1} \min_{x \in [0, C]^k} \frac{1}{2} \|x\|_{K(\theta)}^2 - 1^T x, \quad x^T y = 0.$$

This problem was solved in [19] by using variable projection in  $x$ , with the outer problem in  $\theta$  solved by the prox-gradient method. The scheme is inefficient, since each step in  $\theta$  requires a full QP solve in  $x$ . To develop a faster algorithm, we instead project out  $\theta$  (which has a closed form solution), and iterate in  $x$ .

### C. Trimmed Formulations in Machine Learning

Many formulations in high-dimensional regression, machine learning, and statistical inference are formulated as minimization problems

$$\min_x \sum_{i=1}^n f_i(x) + r(x),$$

where the training set comprises  $n$  examples,  $f_i$  is the error/loss corresponding to the  $i$ th training point, and  $r(x)$  is a regularizer.

All of these formulations can be made robust to perturbations of input data (for example, incorrect features, gross outliers, or flipped labels) using a *trimming approach*. The idea, first proposed by [21] for least

problem	known parameters	unknown parameters	$\varphi_{ij}$
pharmaco-kinetic	time $t$	decay rate $x$	$x_i t_j$
signal classification	distances $a_j$	direction $x$	$x_i a_j$
radial basis functions	locations $a_j$	center $x$ and scale $\theta$	$\theta_i^2 \ a_j - x_i\ _2^2$

TABLE I: Some examples of exponential data-fitting in applications.

squares fitting, is to minimize the  $N < n$  smallest residuals. The general trimmed approach, formulated and studied in [2], [33], considers the equivalent formulation

$$\min_{x, \theta} \sum_{i=1}^n \theta_i f_i(x) + r(x), \quad \theta \in \hat{\Delta}_N. \quad (6)$$

Here, the set  $\hat{\Delta}_N := \{\theta_i \in [0, 1], \quad 1^T \theta = N\}$  is called the *capped simplex*, and admits an efficient projection operator [2]. Jointly solving for  $(x, \theta)$  simultaneously detects the  $N$  inliers as the model  $x$  is fit; the user provides a value  $N \leq n$ . The reader can check that the solution in  $\theta$  for fixed  $x$  selects the smallest  $N$  terms  $f_i$ . The problem therefore looks like a good candidate for VP. The difficulty is that the projected function  $\tilde{f}(x)$  is typically highly nonsmooth; see Fig. 1.

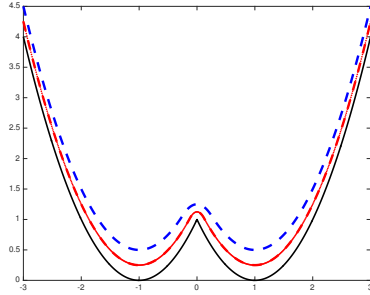


Fig. 1:  $f_1(x) = (x-1)^2$  and  $f_2(x) = (x+1)^2$ . The resulting function  $\min\{f_1, f_2\}$  is nonsmooth at the origin (black solid curve). The effect of smoothing (7) is shown in dashed blue for  $\beta = 1$ , and dash-dot red for  $\beta = 0.5$ .

By introducing smoothing in  $\theta$ , we can apply VP, and optimize the projected function efficiently using a Quasi-Newton method. The smoothed formulation is given by

$$\min_{x, \theta \in \hat{\Delta}_N} \sum_{i=1}^n f_i(x) \theta_i + r(x) + \frac{\beta}{2} \|\theta\|^2. \quad (7)$$

We show that for batch problems, this approach can be orders of magnitude faster than first-order methods for the robust trimming problem.

To apply numerical methods to the function  $\tilde{f}$  or its approximation  $\tilde{f}_\beta$ , we must understand when the two functions are smooth. This is the content of the following section.

### III. DERIVATIVE FORMULAS AND INEXACT VP

In this section, we present differentiability conditions, derivative formulas, and develop a numerical approach based on VP for problems of the form (1).

#### A. Derivatives and Partial Minimization

Let us first briefly recap two standard definitions. A function  $f: \mathbb{R}^n \rightarrow \mathbb{R}$  is *differentiable* at  $\bar{x}$  if there exists a vector  $v$ , called the *gradient* and denoted  $\nabla f(\bar{x})$ , satisfying

$$\lim_{y \rightarrow \bar{x}} \frac{f(y) - f(\bar{x}) - \langle v, y - \bar{x} \rangle}{\|y - \bar{x}\|} = 0.$$

A function  $f$  that is differentiable at  $\bar{x}$  is *strictly differentiable* at  $\bar{x}$  if it satisfies the slightly stronger property

$$\lim_{z, x \rightarrow \bar{x}} \frac{f(z) - f(x) - \langle \nabla f(\bar{x}), z - x \rangle}{\|z - x\|} = 0.$$

Strict differentiability, in particular, implies local Lipschitz continuity of the function, in contrast to conventional differentiability [20, Theorem 9.18].

The following fundamental result [20, Theorem 10.58] helps establish strict differentiability and derivative formulas for *value functions*, i.e. those obtained by the variable projection technique.

**Theorem 1** (Derivative of the value function). *Consider a function  $f: \mathbb{R}^k \times \mathbb{R}^n \rightarrow \mathbb{R}$  satisfying the following properties*

- 1)  $f$  is continuous;
- 2)  $f(x, \theta)$  is level-bounded in  $\theta$  locally uniformly in  $x$ , meaning that for any  $\alpha \in \mathbb{R}$  and any compact set  $X \subset \mathbb{R}^n$ , the union of sublevel sets  $\bigcup_{x \in X} \{\theta : f(x, \theta) \leq \alpha\}$  is bounded.
- 3) gradient  $\nabla_x f(x, \theta)$  exists for all  $(x, \theta)$  and depends continuously on  $(x, \theta)$ .

Denote the projected function and the minimizing set as

$$\tilde{f}(x) := \inf_{\theta} f(x, \theta) \quad \text{and} \quad \vartheta_x := \operatorname{argmin}_{\theta} f(x, \theta).$$

Then  $\tilde{f}$  is strictly differentiable at any point  $x$  for which the set  $\mathcal{D}_x := \{\nabla_x f(x, \theta) : \theta \in \vartheta_x\}$  is a singleton, and in this case we have  $\nabla \tilde{f}(x) = \mathcal{D}_x$ .

There are some important limitations of Theorem 1. The theorem does not immediately apply to all the problems of interest; indeed,  $\theta$  may vary over a constrained set, and therefore properties 1 and 3 fail, since

$f$  then takes infinite values. In structured circumstances, however, one can correct for that either by representing the function  $\tilde{f}$  in a more convenient form (through dual variables) or by instead considering the regularized function  $\tilde{f}_\beta$ . We discuss both of these techniques in Section IV.

When the inner problems can be solved quickly, we use these results to design competitive methods for

$$\min_x \tilde{f}(x) + r(x). \quad (8)$$

When  $r$  is smooth, we can apply a gradient-based method

$$x_{k+1} = x_k - \alpha_k (\nabla \tilde{f}(x_k) + \nabla r(x_k)).$$

When  $r$  is not smooth, but admits a computable proximity operator,

$$\text{prox}_{\alpha r}(x) = \underset{y}{\operatorname{argmin}} \left\{ r(y) + \frac{1}{2\alpha} \|x - y\|^2 \right\},$$

we can apply a proximal gradient algorithm

$$x_{k+1} = \text{prox}_{\alpha_k r}(x_k - \alpha_k \nabla \tilde{f}(x_k)).$$

In many applications, the inner problem does not have a closed-form solution, and must be solved with an iterative scheme. To make the algorithms efficient, it is desirable to stop the inner computation early, yielding inexact gradients of the projected function  $\tilde{f}$ . In the next section we derive bounds on the error in the gradient and propose an inexact gradient method for solving the outer problem.

### B. Inexact Gradients

An evaluation of  $\tilde{f}$  requires solving

$$\tilde{f}(x) = \min_{\theta} g(x, \theta) + h(\theta). \quad (9)$$

When this objective is convex, we can easily control the degree of inexactness, and adapt it to the outer algorithm for minimizing  $\tilde{f}(x)$ . Here, we make these notions precise, assuming that  $g$  is strongly convex in  $\theta$ , while  $h$  is convex and admits a proximity operator. Then for each  $x$ , the subproblem (9) has a unique solution  $\theta(x)$ , and we can use a linearly convergent algorithm to find it. For example, a basic proximal-gradient method generates iterates  $\theta_k$  satisfying

$$\|\theta_k - \theta(x)\|^2 \leq (1 - \kappa(x))^k \|\theta_0 - \theta(x)\|^2, \quad (10)$$

where  $\kappa(x)$  is the reciprocal of the condition number of  $g(x, \cdot)$ . Assuming that  $\kappa(\cdot)$  is uniformly bounded below by some  $\kappa > 0$ , over all  $x$ , the number of iterations required to achieve  $\epsilon$  accuracy is  $\kappa^{-1} \mathcal{O}(\log \epsilon^{-1})$ , ignoring initialization.

When the hypotheses of Theorem 1 are satisfied, the function  $\tilde{f}$  in (9) is smooth and its gradient is given by  $\nabla \tilde{f}(x) = \nabla_x g(x, \theta(x))$ . We can bound the error

between the gradient obtained using  $\theta_k$  as an approximation of  $\theta(x)$  by

$$\|\nabla_x g(x, \theta_k) - \nabla_x g(x, \theta(x))\| \leq C_x \|\theta_k - \theta(x)\|, \quad (11)$$

where  $C_x$  is the Lipschitz constant of  $\nabla_x g(x, \cdot)$ .

Combining (10) and (11), we can obtain inexact gradients up to any given error level. This opens the door to a range of inexact-gradient methods for solving problems of the form (8), including inexact proximal gradient methods [25] or smooth optimization with an inexact oracle [9]. We take advantage of the fast rates of convergence to adapt the error level of the inner problem to the convergence rate of a first-order algorithm for  $\tilde{f}$ , detailed in Algorithm 1. The algorithm uses an InnerSolver, which is a fast first-order method for smooth convex problems with simple regularizers. The stepsizes  $\alpha_k$  are (local) estimates of the reciprocal Lipschitz constant of  $\nabla_x g(\cdot, \theta_k)$ . A detailed analysis of the global complexity of this approach for a wide class of problems, motivated by PDE constrained motivation, can be found in [3].

---

#### Algorithm 1 Inexact Nonsmooth VP

---

**Input:**  $x_0 \in \mathbb{R}^k, \theta_0 \in \mathbb{R}^n, g(\cdot, \cdot), h(\cdot), r(\cdot), \eta > \epsilon_0 > 0, \beta < 1$   
1:  $\delta_0 \leftarrow 1$   
2: **while**  $\epsilon_k + \delta_k > \eta$  **do**  
3:    $\theta_{k+1} \leftarrow \text{InnerSolve}(g(x_k, \cdot), h(\cdot), \theta_k, \epsilon_k)$   
4:    $x_{k+1} \leftarrow \text{prox}_{\alpha_k r}[x_k - \alpha_k \nabla_x g(x_k, \theta_k)]$   
5:    $\epsilon_{k+1} \leftarrow \beta \epsilon_k$   
6:    $\delta_{k+1} \leftarrow \|x_{k+1} - x_k\| / \alpha_k$   
7:    $k \leftarrow k + 1$   
**return**  $x_{k+1}, \theta_{k+1}$

---

A simple proximal gradient method for solving the inner problem is detailed in Algorithm 2. Here,  $\alpha_k$  is a (local) estimate of the reciprocal Lipschitz constant of  $\nabla_{\theta} g(\theta_k)$ .

---

#### Algorithm 2 InnerSolver: Proximal Gradient

---

**Input:**  $g(x, \cdot), h(\cdot), \theta_0 \in \mathbb{R}^n, \epsilon > 0$   
1:  $\delta_0 \leftarrow 1$   
2: **while**  $\delta_k > \epsilon$  **do**  
3:    $\theta_{k+1} \leftarrow \text{prox}_{\alpha_k h}(\theta_k - \alpha_k \nabla_{\theta} g(x, \theta_k))$   
4:    $\delta_{k+1} \leftarrow \|\theta_{k+1} - \theta_k\| / \alpha_k$   
5:    $k \leftarrow k + 1$   
**return**  $\theta_{k+1}$

---

A much faster algorithm in practice is the FISTA algorithm [5]. FISTA keeps track of an additional sequence  $\phi_k$  and steps  $t_k$ . FISTA is more efficient in practice than simple proximal gradient, and there are variants that converge linearly at an optimal rate for strongly convex problems [14].



**Algorithm 3** InnerSolver: FISTA**Input:**  $g(x, \cdot), h(\cdot), \theta_0 \in \mathbb{R}^n, \epsilon > 0$ 


---

```

1:  $\delta_0 \leftarrow 1$ 
2:  $\phi_0 \leftarrow \theta_0$ 
3: while  $\delta_k > \epsilon$  do
4:    $\theta_{k+1} \leftarrow \text{prox}_{\alpha_k h}(\phi_k - \alpha_k \nabla f(\phi_k))$ 
5:    $t_{k+1} \leftarrow \frac{1 + \sqrt{1 + 4t_k^2}}{2}$ 
6:    $\phi_{k+1} \leftarrow \theta_{k+1} + \left(\frac{t_k - 1}{t_{k+1}}\right)(\theta_{k+1} - \theta_k)$ 
7:    $\delta_{k+1} \leftarrow \|\theta_{k+1} - \theta_k\| / \alpha_k$ 
8:    $k \leftarrow k + 1$ 
return  $\theta_{k+1}$ 

```

---

Algorithms 2 and 3 are both implemented as options for the InnerSolve in line 3 of Algorithm 1<sup>2</sup>.

## IV. CASE STUDIES

In this section, we provide implementation details and description of competing techniques for the three examples.

First, we compare nonsmooth optimization for direction-of-arrival (DOA) estimation to the classic MUSIC algorithm. We also show that the projected approach has superior performance to joint optimization, and in particular finds a lower objective value for the full nonconvex problem.

Second, we consider a blind deconvolution example, where we add non-negativity constraints.

Third, we test the new MKL approach, using an off-the-shelf SQP solver to optimize the function  $f$ .

Finally, we compare the PALM algorithm [7] for trimming general linear models to variable projection applied to the smoothed trimming problem.

## A. Direction-of-arrival estimation (DOA)

Estimating the direction of arrival is a classic problem in array-based signal processing. Incoming signals from multiple sources (e.g., electromagnetic or acoustic waves) are recorded by an array of receivers. The goal is to identify the directions from which various contributions originated. This problem is solved by exponential data-fitting, with incoming plane waves modeled by a complex exponential

$$y = \Phi(x)\theta + \epsilon,$$

where  $y \in \mathbb{R}^m$  denotes the signal,  $\Phi(x) \in \mathbb{R}^{m \times n}$  is a matrix with elements  $\exp(-ix_j \cdot a_i)$ , the elements  $\theta \in \mathbb{R}^n$  are the amplitudes of the individual components,  $x_j \in \mathbb{S}^1$  are the directions, and  $a_i \in \mathbb{R}^2$  are the locations of the receivers.

<sup>2</sup><https://github.com/UW-AMO/VarProNonSmooth>

The classical way of estimating the parameters  $x_i$  is the MUSIC algorithm [8], [26]. This algorithm proceeds to estimate the DOA as follows. First, treating  $\theta$  and  $\epsilon$  as random variables, define the signal correlation matrix

$$\Sigma_x = \mathbb{E}_\theta \{\Phi(x)\theta\theta^* \Phi(x)^*\},$$

which is an  $m \times m$  matrix with rank  $\min\{m, n\}$ . Let  $P$  be the matrix whose columns span the null-space of  $\Sigma_x$ . The MUSIC pseudo-spectrum is now defined as

$$f(x) = \frac{1}{\|P^*s(x)\|_2},$$

where  $s_i(x) = \exp(ix \cdot a_i)$ . If  $s(x)$  is nearly in the range of  $\Sigma_x$ , its projection onto the null-space is nearly zero, thus causing a large peak in the pseudo-spectrum. The components in the signal can then be detected by taking the  $m$  largest peaks in the pseudo-spectrum.

In practice, true signal correlation is not available, so the sample average is used instead:

$$\Sigma_y \approx \frac{1}{N} \sum_{i=1}^N y_i y_i^*.$$

If  $\epsilon$  is i.i.d. Gaussian with variance  $\sigma$  and independent of  $\theta$ , we have

$$\Sigma_y = \Sigma_x + \sigma^2 I,$$

in which case we construct  $P$  from the singular vectors of  $\Sigma_y$  with singular values smaller than  $\sigma^2$ . Proper identification of the null-space requires an estimate of the noise level.

We compare the MUSIC algorithm to an optimization-based approach, solving

$$\min_{x, \theta} \|\Phi(x)\theta - y\|_2^2 + \lambda \|\theta\|_1. \quad (12)$$

The sparsity-promoting term  $\lambda \|\theta\|_1$  is included to discover a small set of candidate sources automatically. The reader can immediately verify that assumptions 1 and 3 of Theorem 1 hold. To ensure assumption 2 holds, we must assume either that  $\Phi(\theta)$  has full column rank for all  $x$  or add a quadratic term  $\beta \|\theta\|_2^2$  to the objective (12).

An example with  $N = 10$ ,  $n = 101$  and  $m = 5$  is shown in figure 2. Note that the observed data contains arrivals from only 3 distinct directions. We solved the VP subproblems (LASSO) using an accelerated proximal gradient method while using a Quasi-Newton method to minimize  $\tilde{f}$ . We compare this VP approach to solving the full optimization problem in  $(\theta, x)$  jointly using a non-smooth Quasi-Newton method [12].

The observed and fitted data are shown in figure 2 (a) and the true and estimated DOAs and amplitudes as well as the MUSIC spectrum are shown in figure 2 (b). The MUSIC spectrum picks up the strongest modes but fails to recover the weaker mode. Solving the optimization problem correctly recovers directions and amplitudes of

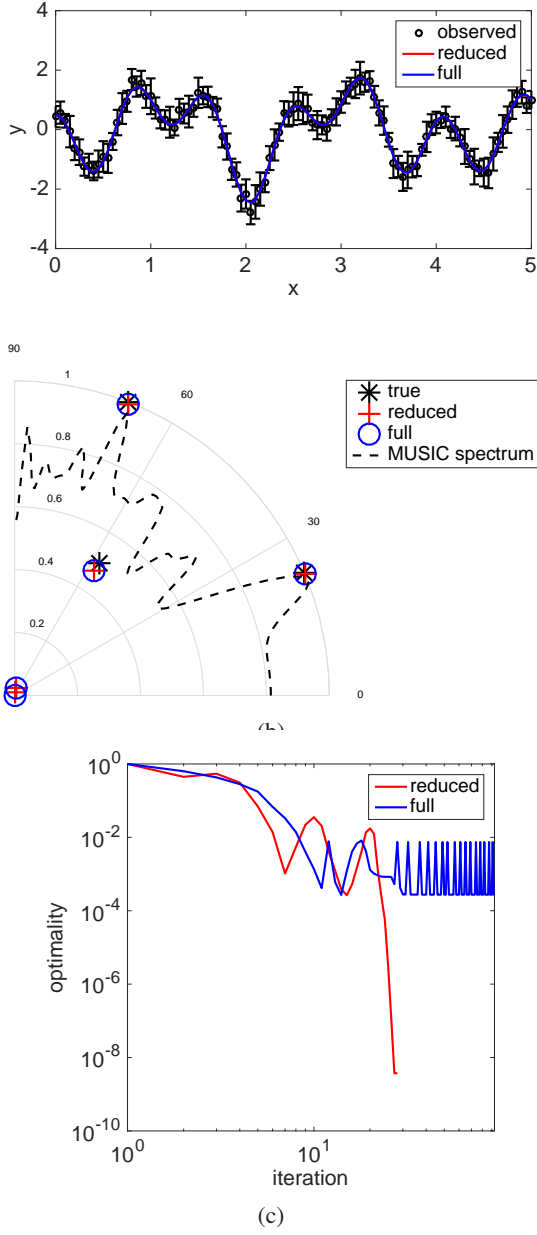


Fig. 2: DOA results: (a) observed and fitted data, (b) true and estimated direction-of-arrival and corresponding amplitudes, as well as the MUSIC spectrum, and (c) convergence of the full and reduced approach.

all 3 arrivals. The solutions returned by two algorithms (nonsmooth BFGS and variable projection) are in close agreement. However, the new approach converges to an accurate solution, while the full approach fails to decrease the measure of stationarity past  $10^{-4}$  (2 (c)).

We repeated the above experiment for 100 different initial guesses and summarized the results in terms of the number of iterations required to reach the desired tolerance of  $10^{-6}$  and optimality (relative norm of the

gradient) in figure 3. We see that the reduced approach almost always reaches the desired tolerance and requires less iterations to do so. In contrast, the full approach fails to reach the desired tolerance in roughly 35/100 cases.

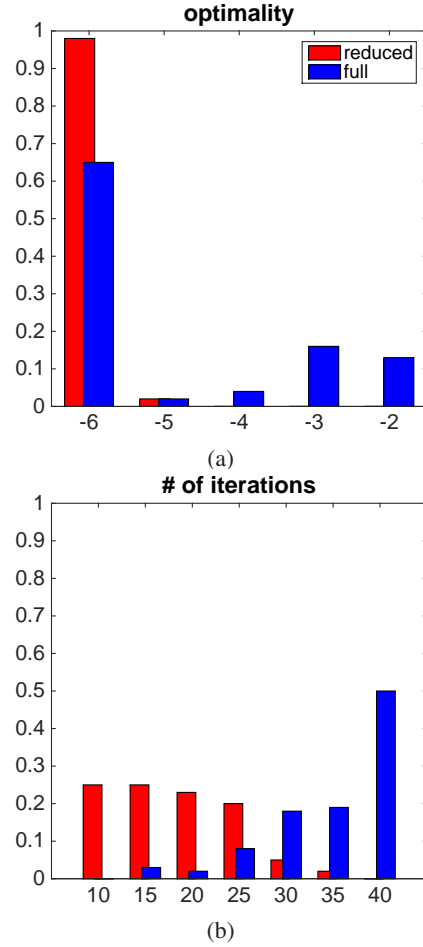


Fig. 3: Results of VP versus full-space optimization for 100 different initial guesses, with a required tolerance of  $10^{-6}$ . (a) shows the relative tolerance upon convergence (or failure) of the optimization, (b) shows the number of iterations required by both methods. We see that the reduced approach almost always reaches the desired tolerance and requires less iterations than the full approach.

### B. Blind sparse deconvolution: full vs. reduced

Next, we consider a parametrized blind deconvolution problem. We are given a noisy image which we want to decompose into a number of parametrized basis functions. Such problems occur often in astrophysics [29], image deblurring [1], [17] and seismology [13], [22].

In this case, letting  $x = (r, s)$ , we have  $\varphi_{ij}(x) = \exp(-s_j^2 \|a_i - r_j\|_2^2)$  and formulate the problem as

$$\min_{x, \theta \geq 0} \frac{1}{2} \|\Phi(x)\theta - y\|^2 + \lambda \left( \|\theta\|_1 + \frac{1}{2} \|\theta\|^2 \right). \quad (13)$$

The non-negative elastic net regularization (in parenthesis on (13)) looks for sparse non-negative linear combinations of signals that explain the data. Unfortunately, the constraint  $\theta \geq 0$  violates assumptions of Theorem 1. Thus we do not a priori know if the projected function  $\tilde{f}$  is even differentiable. To rectify this difficulty, we will see that the dual of the problem  $\min_{\theta} f(x, \theta)$  up to a sign flip is equal to  $-\min_{\phi} g(x, \phi)$ , where  $g$  does satisfy the required hypotheses. Denote the sum of the constraint and elastic net penalty by  $k(\theta)$ :

$$k(\theta) = \lambda \left( \|\theta\|_1 + \frac{1}{2} \|\theta\|^2 \right) + \delta_{\mathbb{R}_+^n}(\theta).$$

The convex conjugate (see e.g. [20]) is given by

$$k^*(z) = \frac{1}{2\lambda} \text{dist}^2(z | (-\infty, \lambda]^n),$$

and is a differentiable function. Treating  $x$  as fixed and dualizing in  $\theta$ , the dual objective to (13) (see e.g. [20, Example 11.41]) is given by

$$g(x, \phi) = \frac{1}{2} \|\phi - y\|^2 + \frac{1}{2\lambda} \text{dist}^2(\Phi(x)^T \phi | (-\infty, \lambda]^n),$$

where  $\phi$  is a dual variable. Notice that  $g$  now satisfies all hypotheses of Theorem 1.

When the regularizer is  $\lambda \|\theta\|_1$  rather than the elastic net, existence of derivatives requires the additional assumption that  $\Phi(x)^T \Phi(x)$  is uniformly positive definite in  $x$ , in which case by an analogous computation we get

$$g(x, \phi) = \frac{1}{2\lambda} \text{dist}_{(\Phi^T \Phi)^{-1}}^2(\phi | (-\infty, \lambda]^n) - \langle y, \phi \rangle.$$

The outer optimization over  $x$  is done using a Quasi-Newton method. We compare the VP approach to a full optimization over the  $(\theta, x)$ -space. The results are shown in figure 4. The ground truth image consists of four blobs; the initial guess for  $r$  is obtained by picking the 50 largest peaks in the noisy image. The reconstructions obtained by the VP and full approaches look similar, but we see that the full approach has trouble getting rid of the superfluous points. The convergence plots, shown in figure 5, show that the full approach does not fit the data as well as the VP approach and converges very slowly.

### C. Fast MKL using variable projection

In this example, we show how variable projection can be used for Multiple Kernel Learning (MKL). Rather than minimizing out the  $x$  variable, consider minimizing in  $\theta$  instead:

$$\min_{x \in [0, C]^k} \tilde{f}_{\beta}(x) - 1^T x \quad \text{s.t.} \quad x^T y = 0, \quad (14)$$

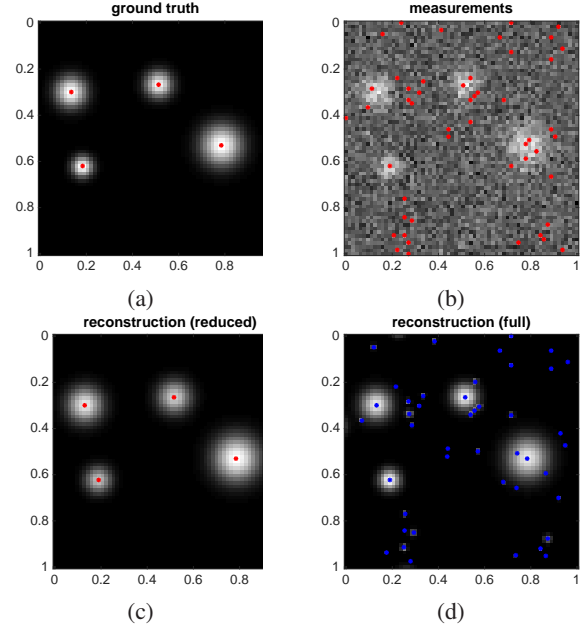


Fig. 4: (a) ground truth image, (b) noisy image and initial guess for  $r$ , (c) results using the VP approach, and (d) results using the full approach.

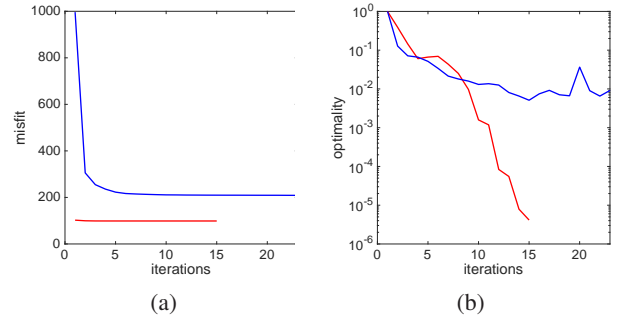


Fig. 5: Convergence of the full and reduced approaches in terms of the misfit (a) and the optimality (b) for blind sparse deconvolution.

and

$$\begin{aligned} \tilde{f}_{\beta}(x) &= \min_{\theta \in \Delta_1} \sum_i \theta_i \underbrace{\langle K_i x, x \rangle}_{f_i(x)} + \frac{\beta}{2} \|\theta\|^2 \\ &= \min_{\theta \in \Delta_1} \frac{\beta}{2} \|\theta - (-f(x)/\beta)\|^2 - (2\beta)^{-1} \|f(x)\|^2 \\ &= \frac{\beta}{2} \text{dist}_{\Delta_1}^2(-f(x)/\beta) - (2\beta)^{-1} \|f(x)\|^2, \end{aligned} \quad (15)$$

where to go from the second to the third line of (15) we partially minimize in  $\theta$ , obtaining

$$\theta(x) = \text{proj}_{\Delta_1}(-f(x)/\beta).$$

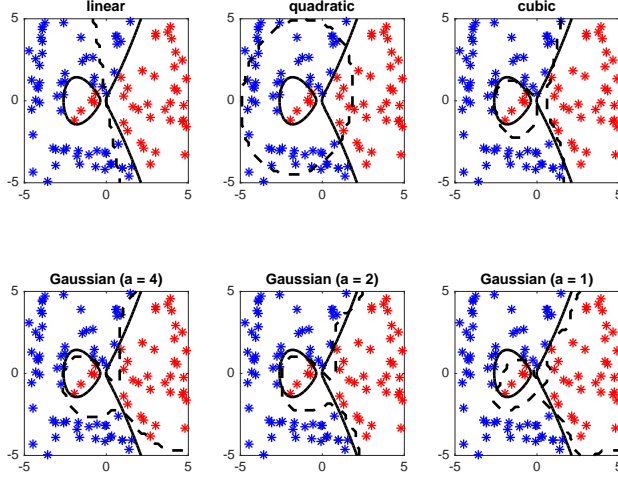


Fig. 6: Classification of points in the plane using different kernels. The red and blue stars indicate the training set, the solid line denotes the elliptic curve used to separate the points and the dotted line shows the classification resulting from the optimization procedure.

The term  $\frac{\beta}{2}\|\theta\|^2$  is required to ensure the existence of a derivative, which is given by (see the first line of (15))

$$\nabla \tilde{f}_\beta(x) = \sum_i \theta_i(x) \nabla f_i(x).$$

Standard approaches can now be applied to solve (14) with the modified  $\tilde{f}_\beta$ . In our numerical examples, we show that the complexity of this approach is essentially equivalent to solving a single kernel learning problem.

We solve the smoothed dual problem (14) using sequential quadratic programming (SQP) with approximate Hessian  $H = \sum_i \theta_i K_i$ . We consider two parametrized classes of kernel functions, polynomial and Gaussian:

$$k_p^{\text{pol}}(a, a') = \left(1 + a^T a'\right)^p,$$

$$k_s^{\text{Gauss}}(a, a') = \exp(-\|a - a'\|_2^2 / \sigma^2).$$

To illustrate the approach, we classify points in  $\mathbb{R}^2$  to the left and to the right of an elliptic curve. In figure 6, we show the results for various kernels. In table II, we show the number of iterations required for each kernel.

In figure 7 we show the result using a total of 12 kernels; 5 polynomial kernels with  $p = 1, 2, \dots, 5$  and 7 Gaussian kernels with parameters  $\sigma = 1, 1.5, 2, \dots, 4$ . Our approach quickly hones in on the Gaussian kernel with  $\sigma = 1$  and takes a total of 107 iterations.

kernel	1	2	3	4	5	6
iterations	30	33	21	94	57	45

TABLE II: Number of iterations required for the results shown in figure 6.

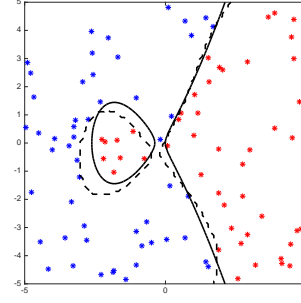


Fig. 7: Classification of points in the plane using the new multiple kernel learning approach.

#### D. Trimmed General Linear Models via Quasi-Newton

Suppose we are given training features  $a_i$  and responses  $b_i$  with special restrictions. They may be count data (number of trees that fall over in a storm), indicate class membership (outcome of a medical study, handwritten digit recognition), or be non-negative (concentration of sugar in the blood). These problems and many others can be modeled using *general linear models* (GLMs). Let the distribution of  $b_i$  be parametrized by  $(\mu_i, \sigma^2)$ :

$$L(b_i | \mu_i, \sigma^2) = \rho_1(b_i, \sigma^2) \exp\left(\frac{b_i \mu_i - \rho(\mu_i)}{\rho_2(\sigma^2)}\right).$$

To obtain the GLM, set  $\mu_i := \langle a_i, x \rangle$ , and minimize the negative log-likelihood:

$$\min_x \sum_{i=1}^m \rho(\langle a_i, x \rangle) - b_i \langle a_i, x \rangle,$$

ignoring  $\rho_1$  and  $\rho_2$  as they do not depend on  $x$ . We can recover many common statistical inference problems:

- Linear regression ( $b_i \in \mathbb{R}$ ):  $\rho(z) = \frac{1}{2}\|z\|^2$ .
- Classification ( $b_i \in \{0, 1\}$ ):  $\rho(z) = \log(1 + e^z)$ .
- Poisson regression ( $b_i \in \mathbb{Z}_+$ ):  $\rho(z) = e^z$ .
- Exponential regression ( $b_i \geq 0$ ):  $\rho(z) = -\ln(z)$ .

Following [2], [33], we can formulate a robust version of any GLM:

$$\min_{x, \theta \in \hat{\Delta}_h} \sum_{i=1}^m \theta_i (\rho(\langle a_i, x \rangle) - b_i \langle a_i, x \rangle).$$

This problem is smooth in  $x$  but not smooth in  $\theta$ . The set  $\hat{\Delta}_N := \{\theta_i \in [0, 1], \quad 1^T \theta = N\}$  is the capped simplex. We can therefore apply the PALM algorithm [7] to solve the problem. Let  $f_i(x) := \rho(\langle a_i, x \rangle) - b_i \langle a_i, x \rangle$ . Algorithm 4 gives the PALM iteration for this problem.



**Algorithm 4** Proximal Alternating Linearized Minimization Method (PALM)**Input:**  $x \in \mathbb{R}^d, \theta \in \mathbb{R}^n, h \leq n, \gamma > 0, \tau > 0$ 1: **loop**2:  $\theta \leftarrow \text{prox}_{\tau r_1} \left( \theta - \frac{\tau}{n} (f_1(x), \dots, f_n(x)) \right)$ 3:  $x \leftarrow \text{prox}_{\gamma r_2} \left( x - \frac{\gamma}{n} \sum_{i=1}^n \theta_i \nabla f_i(x) \right)$ 

Just as for MKL, we add a small smoothing term  $\frac{\beta}{2} \|\theta\|^2$ , and compute the exact gradient of the modified projected function

$$\begin{aligned} \tilde{f}_\beta(x) &= \min_{\theta \in \hat{\Delta}_h} \sum_{i=1}^m \theta_i \underbrace{(\rho(\langle a_i, x \rangle) - b_i \langle a_i, x \rangle)}_{f_i(x)} + \frac{\beta}{2} \|\theta\|^2 \\ &= \frac{\beta}{2} \text{dist}_{\hat{\Delta}_h}^2 \left( -\beta^{-1} f(x) \right) - \frac{1}{2\beta} \|f(x)\|^2, \end{aligned}$$

by an identical computation to (15), replacing  $\Delta_1$  with  $\hat{\Delta}_h$ . The gradient is  $\nabla \tilde{f}_\beta(x) = \sum_i \nabla f_i(x) \theta_i(x)$ , where

$$\theta(x) = \text{proj}_{\hat{\Delta}_h} (-f(x)/\beta).$$

Projection onto this set has been recently considered and implemented [31]. We compute it using root finding<sup>3</sup>. These results allow standard methods for (7), including prox-gradient for non-smooth  $r(x)$ , provided  $\nabla f$  is Lipschitz continuous, and Quasi-Newton (BFGS) methods [32] when  $r(x)$  is smooth.

We minimize  $\tilde{f}_\beta$  using BFGS, and compare the performance of this algorithm to that of PALM. We consider two cases:

- Continuous data.  $m = 1000$  measurements are generated according to  $y = Ax + \epsilon$ , where  $x \in \mathbb{R}^{100}$  and  $\epsilon$  are Gaussian. 10% of the errors have extremely high variance. We fit a trimmed least squares model

$$\min_{w \in \Delta_h} \sum_{i=1}^m w_i \|\langle a_i, x \rangle - b_i\|^2 + \frac{\beta}{2} \|w\|^2 + \frac{1}{2m} \|x\|^2,$$

and count outliers we correctly detected.

- Binary data. 1000 measurements are generated according to  $y = \text{sign}(Ax + \epsilon) + 1$ , giving observations in  $\{0, 1\}$ . Labels for 10% of the observations are flipped. We fit a trimmed logistic regression problem

$$\min_{w \in \Delta_h} \sum_{i=1}^m w_i LE(\langle a_i, x \rangle - b_i \langle a_i, x \rangle + \frac{\beta}{2} \|w\|^2 + \frac{1}{2m} \|x\|^2)$$

where  $LE(r) = \log(1 + \exp(r))$  and count outliers we correctly detected.

PALM stops when the sum of normalized updates to  $(x, w)$  is smaller than  $1e^{-6}$ , or when the number of

<sup>3</sup> We find  $\lambda$  satisfying  $1^T \text{proj}_{[0,1]}(w - \lambda) = h$ , and then  $w - \lambda$  gives the projection onto  $\hat{\Delta}_h$ .

$\beta = 1$	PALM	BFGS	$\beta = 100$	PALM	BFGS
Time	<b>7.9</b>	<b>0.5</b>	Time	<b>41.3</b>	<b>2.4</b>
Iters	10K	81	Iters	50K	502
Obj	627.5	627.6	Obj	-7.1e4	-4.7e4
Acc.	85%	85%	Acc.	82%	79%
$\beta = .1$	PALM	BFGS	$\beta = 1$	PALM	BFGS
Time	<b>3.24</b>	<b>0.34</b>	Time	<b>15.6</b>	<b>0.49</b>
Iters	5975	55	Iters	50K	287
Obj	281.4	281.1	Obj	-1.14e5	-8.6e4
Acc.	85%	87%	Acc.	83%	81%
$\beta = .01$	PALM	BFGS	$\beta = .01$	PALM	BFGS
Time	<b>2.8</b>	<b>0.33</b>	Time	<b>14.9</b>	<b>0.41</b>
Iters	6018	29	Iters	50K	241
Obj	245	246	Obj	-1.14e5	-8.6e4
Acc.	84%	86%	Acc.	85%	82%

TABLE III: Results for trimmed VP. Left: trimmed least squares. Right: trimmed logistic. BFGS gets comparable accuracy, but finishes far faster than PALM.

iterations reaches 50K. The function  $r_2$  in Algorithm 4 is

$$r_2(w) = \delta_{\Delta_h}(w) + \frac{\beta}{2} \|w\|^2,$$

so  $\beta$  does not affect the Lipschitz constant of the gradient with respect to  $w$ . BFGS stops when the norm of the gradient is smaller than  $1e^{-8}$ ; there is no iteration cap.

Results are presented in Table III. PALM iterations were capped at 50K; there was no cap on BFGS iterations. BFGS is at least 10 times faster than PALM on all examples.

For trimmed least squares, BFGS finds as good or slightly better objective values than PALM. The accuracy of outlier detection of the BFGS approach is at least as good or better than that of PALM. For trimmed logistic regression, BFGS finds worse objective values; however the optimality conditions at the solutions were on the order of  $1e^{-9}$ , so the discrepancy is due to BFGS finding a worse local minimum. Indeed, for this problem, the results flip, and accuracy of outlier detection of PALM is as good or better than that of BFGS. Weight detection using partial minimization may be too aggressive for logistic regression.

In any case, outlier detection accuracies are roughly comparable for the two problems, and for both algorithms. The approach is also robust for different choices of  $\beta$ ; in fact, it seems that larger values of  $\beta$  make the problem harder. For both algorithms, larger  $\beta$  roughly correlates with more iterations. In addition, iterations take more time for larger  $\beta$ , because the projection onto the capped simplex becomes more difficult.

In summary, projecting out  $w$  using a small  $\beta$  and using BFGS on the outer problem gives at least an order of magnitude improvement for robust learning problems. For large-scale problems, we can use L-BFGS instead of BFGS.

## V. CONCLUSIONS

Variable projection has been successfully used in a variety of contexts; the popularity of the approach is largely due to its superior numerical performance when compared to joint optimization schemes. In this paper, we considered a range of nonsmooth applications, illustrating the use of variable projection for sparse deconvolution, direction of arrivals estimation, multiple kernel learning, and trimmed robust inference. We showed that differentiability of the projected function can be understood using basic variational analysis. For trimmed formulations and multiple kernel learning, we showed how the problem can be modified to ensure differentiability of the associated projected functions. Numerical examples in all cases showed that variable projection schemes, when appropriately applied, are highly competitive for a wide range of nonsmooth applications. Code implementing these ideas is available through github<sup>4</sup>.

## ACKNOWLEDGMENT

Research of A. Aravkin was partially supported by the Washington Research Foundation Data Science Professorship. Research of D. Drusvyatskiy was partially supported by the AFOSR YIP award FA9550-15-1-0237 and NSF DMS-1651851. The research of T. van Leeuwen was in part financially supported by the Netherlands Organisation of Scientific Research (NWO) as part of research programme 613.009.032.

## REFERENCES

- [1] M. S. C. Almeida and M. a. T. Figueiredo. Parameter estimation for blind and non-blind deblurring using residual whiteness measures. *IEEE Transactions on Image Processing*, 22(7):2751–2763, 2013.
- [2] A. Aravkin and D. Davis. A SMART Stochastic Algorithm for Nonconvex Optimization with Applications to Robust Machine Learning. *arXiv preprint arXiv:1610.01101*, 2016.
- [3] A. Aravkin, D. Drusvyatskiy, and T. van Leeuwen. Quadratic penalization through the variable projection technique. *Preprint arXiv:1606.02395*, 2016.
- [4] A. Y. Aravkin and T. van Leeuwen. Estimating nuisance parameters in inverse problems. *Inverse Problems*, 28(11):115016, nov 2012.
- [5] A. Beck and M. Teboulle. A fast iterative shrinkage-thresholding algorithm for linear inverse problems. *SIAM journal on imaging sciences*, 2(1):183–202, 2009.
- [6] B. Bell and J. Burke. Algorithmic differentiation of implicit functions and optimal values. In C. H. Bischof, H. M. Bücker, P. D. Hovland, U. Naumann, and J. Utke, editors, *Advances in Automatic Differentiation*, pages 67–77. Springer, 2008.
- [7] J. Bolte, S. Sabach, and M. Teboulle. Proximal alternating linearized minimization for nonconvex and nonsmooth problems. *Mathematical Programming*, 146(1-2):459–494, 2014.
- [8] M. Cheney. The linear sampling method and the MUSIC algorithm. *Inverse Problems*, 17(4):S91–S95, 2001.
- [9] O. Devolder, F. Glineur, and Y. Nesterov. First-order methods of smooth convex optimization with inexact oracle. *Mathematical Programming*, 146(1-2):37–75, 2014.
- [10] G. Golub and V. Pereyra. The differentiation of pseudo-inverses and nonlinear least squares which variables separate. *SIAM J. Numer. Anal.*, 10(2):413–432, 1973.
- [11] G. Golub and V. Pereyra. Separable nonlinear least squares: the variable projection method and its applications. *Inverse Problems*, 19(2):R1, 2003.
- [12] A. S. Lewis and M. L. Overton. Nonsmooth optimization via quasi-Newton methods. *Mathematical Programming*, 141(1-2):135–163, oct 2013.
- [13] T. T. Y. Lin and F. J. Herrmann. Robust estimation of primaries by sparse inversion via one-norm minimization. *Geophysics*, 78(3):R133–R150, 2013.
- [14] Y. Nesterov. Gradient methods for minimizing composite functions. *Math. Program.*, 140(1, Ser. B):125–161, 2013.
- [15] M. Osborne. Separable least squares, variable projection, and the Gauss-Newton algorithm. *Electronic Transactions on Numerical Analysis*, 28(2):1–15, 2007.
- [16] D. P. O’Leary and B. W. Rust. Variable projection for nonlinear least squares problems. *Computational Optimization and Applications*, 54(3):579–593, apr 2013.
- [17] S. U. Park, N. Dobigeon, and A. O. Hero. Semi-blind sparse image reconstruction with application to MRFM. *IEEE Transactions on Image Processing*, 21(9):3838–3849, 2012.
- [18] V. Pereyra and G. Scherer, editors. *Exponential Data Fitting and its Applications*. Bentham Science and Science Publishers, mar 2012.
- [19] A. Rakotomamonjy, F. Bach, S. Canu, and Y. Grandvalet. More efficiency in multiple kernel learning. In *Proceedings of the 24th international conference on Machine learning*, pages 775–782. ACM, 2007.
- [20] R. Rockafellar and R. Wets. *Variational Analysis*, volume 317. Springer, 1998.
- [21] P. J. Rousseeuw. Least Median of Squares Regression. *Journal of the American statistical association*, 79(388):871–880, 1984.
- [22] A. A. Royer, M. G. Bostock, and E. Haber. Blind deconvolution of seismograms regularized via minimum support. *Inverse Problems*, 28(12):125010, dec 2012.
- [23] A. Ruhe and P. Wedin. Algorithms for separable nonlinear least squares problems. *SIAM Rev.*, 22(3):318–337, 1980.
- [24] S. Saitoh. *Theory of reproducing kernels and its applications*, volume 189 of *Pitman Research Notes in Mathematics Series*. Longman Scientific & Technical, Harlow; copublished in the United States with John Wiley & Sons, Inc., New York, 1988.
- [25] M. Schmidt, N. L. Roux, and F. R. Bach. Convergence rates of inexact proximal-gradient methods for convex optimization. In *Advances in neural information processing systems*, pages 1458–1466, 2011.
- [26] R. Schmidt. Multiple emitter location and signal parameter estimation. *IEEE Transactions on Antennas and Propagation*, 34(3):276–280, mar 1986.
- [27] B. Schölkopf, R. Herbrich, and A. Smola. A generalized representer theorem. In *Computational learning theory (Amsterdam, 2001)*, volume 2111 of *Lecture Notes in Comput. Sci.*, pages 416–426. Springer, Berlin, 2001.
- [28] B. Schölkopf and A. J. Smola. *Learning with kernels: Support vector machines, regularization, optimization, and beyond*. MIT press, 2002.
- [29] P. Shearer and A. C. Gilbert. A generalization of variable elimination for separable inverse problems beyond least squares. *Inverse Problems*, 29(4):045003, Apr. 2013.
- [30] A. J. Smola and B. Schölkopf. A tutorial on support vector regression. *Statistics and computing*, 14(3):199–222, 2004.
- [31] W. Wang and M. A. Carreira-Perpinán. Projection onto the probability simplex: An efficient algorithm with a simple proof, and an application. *arXiv preprint arXiv:1309.1541*, 2013.
- [32] S. Wright and J. Nocedal. Numerical optimization. *Springer Science*, 35:67–68, 1999.
- [33] E. Yang, A. Lozano, and A. Aravkin. High-Dimensional Trimmed Estimators: A General Framework for Robust Structured Estimation. *arXiv preprint arXiv:1605.08299*, 2016.

<sup>4</sup><https://github.com/UW-AMO/VarProNonSmooth>